Delft University of Technology

Biomedical Engineering
ME51035

The effect of uncertainty in tendon slack length on knee joint reaction force estimations in gait analysis

A thesis submitted to the Delft University of Technology in partial fulfillment of the requirements for the degree of Master of Science in Biomedical Engineering.

Céline Lohmeijer (5826144)

February 6, 2025

Thesis committee:

Prof. dr. ir. J. Harlaar (supervisor)
Dr. M.G.H. Wesseling (daily supervisor)
Dr. M. van der Krogt

Faculty of Mechanical Engineering
February, 2024 - February, 2025

Preface

Growing up, I had no clear career path in mind, but I was absolutely certain about one thing: becoming an engineer was not part of the plan. Well... here we are.

Many years ago, I started the Bachelor's in Human Movement Sciences at the Rijksuniversiteit Groningen. I had been intrigued by human movement for years and this study suited me perfectly. Even though the topic of this thesis is not far from human movement sciences, the educational path that led me to this graduation project has been atypical. I enjoyed my first year of study, but I enjoyed being a student even more and inevitably another bachelor needed to be chosen. After years of dragging myself to lectures during this bachelor, I finally regained interest in studying when I started the master Biomedical Engineering. While the perspective became considerably more technical, my passion for analyzing human movement remained. My enthusiasm in this field may have made this project particularly challenging—when you want to understand everything, where do you draw the line? Nevertheless, I am incredibly grateful for the opportunity to be part of this research group.

I would like to express my gratitude to my supervisors. Mariska, thank you for your guidance throughout this project. You were always willing to make time for me and your open attitude taught me that sometimes the best way to understand new things is to acknowledge that you don't understand it in the first place. Jaap, thank you for your enthusiasm and energy during the biweekly meetings. It was truly inspiring to be a part of that. I also want to thank the other people from the Clinical Biomechanics group. It was nice to share the highs and lows during this project. I (almost) always went home with a smile and some renewed sense of energy.

At last, I want to thank my family for the support along this long educational rollercoaster. Your trust and patience made me believe in myself, even if things were rough. We sang happily "alle 1'tjes zwemmen in het water" after another not-so-successful exam period. Mom and dad, I am very grateful to have had the time to rediscover my passion. A special thanks to my brother who prioritized my coding scripts over his own job. You made me realize that quick fixes don't exist and learning new things is always the better long term solution. Wies, we've been on this rollercoaster together and I don't now where I would have ended up without you, thanks!

Céline
February, 2025

Abstract

Knee osteoarthritis (KOA) is one of the most prevalent joint disease worldwide. Musculoskeletal modeling (MSM) provides a useful tool to investigate knee joint biomechanics and potential development and progression of KOA. However, for clinical usage, it is crucial to understand how patient-specific properties affect MSM outcomes. This study investigated how uncertainty in the tendon slack length (TSL) of lower limb muscles affect knee joint reaction forces (JRFs) in gait analysis. Two sensitivity analyses were performed, one approach used reported TSL variation in literature and the other approach used a percentage TSL variation. Anatomical variation was investigated through a literature review. The JRF estimations of both approaches together resulted in a maximum variation of 0.27 x BW in AP direction, 2 x BW in SI direction and 0.13 x BW in ML direction. Maximum JRF estimations resulting from reported TSL variation were larger in the loading response in all direction. Maximum JRF estimations in ML direction were resulting from percentage variation. TSL of muscles that were found to be most influential in JRF estimations were medial gastrocnemius, rectus femoris, vastus lateralis and psoas. This research confirmed that within patient-specific MSM for clinical purposes, uncertainty in TSL should be limited. Future research should aim to investigate how this influences AC degeneration for KOA.

Contents

Nomenclature

AC - Articular cartilage

ACLR - Anterior cruciate ligament rupture

add_brev - Adductor Brevis

add_long - Adductor Longus

add_mag1 - Adductor Magnus 1 (proximal)

add_mag2 - Adductor Magnus 2

add_mag3 - Adductor Magnus 3 (distal)

bifemlh - Biceps Femoris-Long Head

bifemsh - Biceps Femoris-Short Head

BW - Body weight

DoF - Degree of Freedom

ECM - Extracellular matrix

ercspn - Erector Spinae

ext_dig - Extensor Digitorum Longus

ext_hal - Extensor Hallucis Longus

FEM - Finite Element Modeling

flex_dig - Flexor Digitorum Longus

flex_hal - Flexor Hallucis Longus

gem - Fixme Gem

glut_max1 - Gluteus Maximus 1 (lateral/superior)

glut_max2 - Gluteus Maximus 2

glut_max3 - Gluteus Maximus 3 (medial/inferior)

glut_med1 - Gluteus Medius 1 (anterior)

glut_med2 - Gluteus Medius 2

glut_med3 - Gluteus Medius 3 (posterior)

glut_min1 - Gluteus Minimus 1 (anterior)

glut_min2 - Gluteus Minimus 2

glut_min3 - Gluteus Minimus 3 (posterior)

grac - Gracilis

IK - Inverse Kinematics

iliacus - Iliacus

intobl - Internal Oblique

JRF - Joint reaction force

KOA - Knee Osteoarthritis

lat_gas - Lateral Gastrocnemius

LHS - Latin Hypercube Sampling

med_gas - Medial Gastrocnemius

MS - Musculoskeletal

MSM - Musculoskeletal Modeling

OFL - Optimal fiber length

pect - Pectineus

per_brev - Peroneus Brevis

per_long - Peroneus Longus

per_tert - Peroneus Tertius

peri - Piriformis

quad_fem - Quadratus Femoris

rect_fem - Rectus Femoris

sar - Sartorius

semimem - Semimembranosus

semiten - Semitendinosus

SO - Static optimization

TF - Tibiofemoral

tfl - Tensor Fasciae Latae

tib_ant - Tibialis Anterior

tib_post - Tibialis Posterior

TSL - Tendon slack length

vas_int - Vastus Intermedius

vas_lat - Vastus Lateralis

vas_med - Vastus Medialis

1 Introduction

1.1 Knee osteoarthritis

Knee osteoarthritis (KOA) is one of the most prevalent joint diseases affecting more than 365 million people worldwide in 2019 [1]. Osteoarthritis is a degenerative joint condition, causing pain, swelling and stiffness leading to reduced mobility of the joint [2] [3]. As a consequence, muscles surrounding the affected joint loose strength and patients could become less able to perform physical activities, resulting in decreased well-being and psychological distress [1]. KOA is characterized by degenerative changes in morphology and mechanical properties of articular cartilage (AC) in the knee joint. The main risk factors for KOA are obesity, aging, sex or joint trauma. Age-related changes, inflammatory signals or increased body weight could result in abnormal mechanical stress of AC in the knee joint. This leads to disrupted functionality of chondrocytes which are responsible for producing and maintaining extracellular matrix (ECM) in AC [3]. Distorted production and maintenance of ECM results in loss of integrity of the AC tissue, leading to irreversible damage in the tibiofemoral (TF) bone structure.

Detection of osteoarthritis can be challenging and is most often done through physical examination or radiography [4] [5]. Treatments include physical therapy to regain muscle strength and mobility, and weight loss to reduce knee joint loading. Medications could help to manage pain and swelling resulting from inflammatory responses caused by cartilage degeneration. Gait pattern modifications could aid to reduce knee malalignment responsible for abnormal mechanical stress and knee joint distraction can contribute to the regenerative process of AC [6, 7]. As a last resort, total or partial knee joint replacement could aid to reduce pain and regain mobility. However, this is a severe and expensive surgery requiring months of recovery. Moreover, most artificial knees need to be replaced after 10-20 years making this intervention not optimal for younger patients [8].

In summary, treatments for KOA have their limitations, making prevention or early detection of osteoarthritis crucial to minimize AC degeneration in an early stage. However, this is challenging considering the gradual progression of cartilage degeneration and its vague symptoms. Consequently, understanding biomechanics of the knee joint and how this potentially leads to development of KOA is of great importance.

1.2 Biomechanics

Knee joint loading is determined by the biomechanical behavior of the human body, which depends on many factors including body weight, bone morphology, muscle and ligament properties [3]. The forces within the musculoskeletal system resulting from the interaction between these factors can be analyzed using musculoskeletal modeling (MSM). MSM is a useful non-invasive tool to investigate joint biomechanics through computational analysis of human movement data using motion capture [9]. From marker data, the joint angles during a movement can be obtained, providing the input for estimation of muscle and joint reaction forces (JRF) [10] [11].

The joint biomechanics that can be investigated through MSM are determined by underlying morphology and alignment of the bone, as well as the anatomy and mechanical properties of the muscles and ligaments surrounding the knee [12] [13]. Anatomical characteristics of bone and muscles can to a certain extent be determined using medical imaging [14]. Muscle's volume and cross-sectional area can be determined using MRI and ultrasound. X-rays and CT-scans can be used to estimate bone shape, alignment and bone density [15]. In contrary with anatomical characteristics, mechanical parameters are also influential in muscle functionality. Unfortunately, estimating mechanical parameters in-vivo is very challenging.

1.3 Muscle modeling

Muscle functionality can be described using two concepts: activation and contraction dynamics. Activation dynamics comprises the translation from neural excitation to muscle activation $a(t)$. Contraction dynamics describes the translation from muscle activation to generated muscle force via the force-length-velocity relationship [16]. This relation describes the generated muscle force F^{MT} as a function of the length of the muscle $f(l)$ and the velocity at which the muscle is contracting $f(v)$ (eq. 1).

$$F^{MT} = f_A(\ell)f(\nu)a(t)F_o^m + f_p(\ell)F_o^m\cos(\phi) \tag{1}$$

The relations within in the force-length-relationship are determined by mechanical muscle parameters described in the Hill-type muscle model (fig. 1). According to this model, a muscletendon unit consists of series elastic element (SE), a parallel elastic element (PE) and a contractile element (CE) [17]. The force-length-relationship consists of two components: the active force f_A, generated by the contractile element

in the Hill model, and the passive force component $f_p p$, arising from the parallel element. Within the contractile element, three biomechanical muscle parameters can be distinguished: the maximum muscle force during isometric contraction (maximum isometric force); the muscle fiber length during isometric contraction (optimal fiber length) and the angle between the muscle fibers and the muscle line-of-action (pennation angle ϕ). The series element is the tendon which acts as a passive spring [16]. The biomechanical behavior of the tendon is determined by the tendon slack length (TSL), defined as the length at which the tendon begins to resist stretch and produce force [18].

Estimating mechanical muscle parameters in vivo remains extremely challenging. Existing datasets on muscle parameters are based on cadaveric measurements from decades ago [20]. Over the past few decades, modeling studies have sought to improve the accuracy of muscle parameter estimation using various approaches. However, estimation of muscle parameters are highly interdependent on each other and often rely on simplifications and assumptions [21]. Chen & Franklin (2023) examined the impact of simplifications in muscle parameters estimations on generated muscle force by partially deriving contraction dynamics. Their findings indicate that inaccurate estimates of TSL had the most significant effect on muscle force predictions [21]. Sensitivity analyses focused on gait have also identified TSL as the most influential muscle parameter in muscle force estimations [22, 23, 24, 25, 26]. Based on these comparisons, TSL appears to be the most critical parameter for accurate muscle force estimation in MSM. However, when considering potential cartilage degeneration, JRF estimations are of greater relevance than muscle force alone. Only Navacchia et al. (2016) investigated the impact of muscle parameter uncertainty on knee contact forces while accounting for TSL. Their results suggested that maximum isometric force and muscle attachment points had a greater influence on contact force estimations than TSL [27].

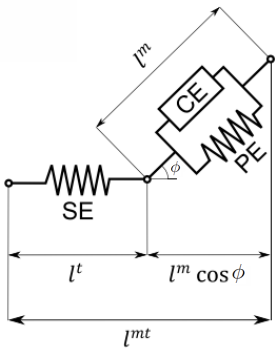

Figure 1: Hill-type muscle model [19]

In summary, while the impact of TSL uncertainty on muscle force is well established, its effect on JRF estimations remains unproven. Additionally, most MSM studies rely on generic models, where muscle parameters are scaled linearly based on subject measurements. In sensitivity analyses, TSL values are typically perturbed by a fixed percentage from their default values. However, this approach is problematic, as default TSL values in generic models are merely estimations and cannot represent the mean TSL for all individuals. In reality, true TSL values remain unknown. This uncertainty is particularly important for clinical applications, where accounting for anatomical variation in muscle parameters is essential for accurate modeling.

1.4 Research objective

Thus, while modeling and simulation techniques provide means to investigate human biomechanics, MS models rely on numerous assumptions about muscle properties. As a result, current MS models are a generalized representation of humans beings, leading to mostly general insights in biomechanical behavior. For clinical application, it is crucial to bridge the gap between generic MSM and personalized MSM to gain insights in patient-specific biomechanics. For investigation of knee JRF for potential development of KOA, the effect of uncertainty in TSL of lower limb muscles should be investigated. To this end, this research aims to answer the research question:

> *"How does uncertainty in tendon slack length affect knee joint reaction force estimations in gait analysis?*

To answer this research question, the anatomical variation reported in literature was compared with the TSL values used in a generic scaled MS model. Two sensitivity analyses were conducted to compare the effect of these different sets of TSL values on JRF estimations during one gait cycle. One experiment used TSL values reported in literature as input variables in a MS model. The other experiment used a percentage perturbation of the default TSL values in a generic MS model. Variation in JRF estimations resulting from the two sets of TSL ranges were analyzed. Resulting muscle force and knee JRF during one gait cycle were analyzed and compared.

It is expected that JRFs variation resulting from TSL variation is large enough to take into consideration for personalized MSM. Muscles most contributing to gait are expected to influence JRF estimations the most.

2 Methods

2.1 Musculoskeletal Model

The MS model Gait2392 in Opensim 4.4 was used to analysis motion capture data. The Gait2392 is a three-dimensional, 23 DoF model of the human musculoskeletal system. It consists of 92 musculotendon actuators representing 76 muscles in the lower extremity and torso, see figure 2. The knee joint in the Gait2392 is a single DoF joint, accounting for the kinematics of both the TF and PF joint in the sagittal plane as well as the patellar levering mechanism [20] [28]. Motion data was provided by Culvenor et al. (2022) within the KOALA cohort in Australia [29]. Gait data were acquired at the University of Melbourne, Australia. The subject was a 21 year old female (weight: 60 kg, height: 173 cm) with history of ACLR surgery in the left knee. The ACL was reconstructed using a single bundle 4-strand semitendinosus and gracilis graft. The model was scaled to measurements of the subject [9].

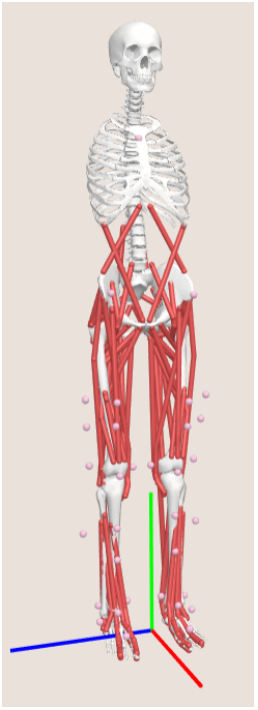

Figure 2: Gait2392 model

The workflow for investigating the effect of uncertainty in TSL on knee JRF estimations can be found in figure 3. Motion marker data was used to perform Inverse kinematics (IK) resulting in joint angles during one gait cycle. The resulting output file was a motion file (.mot) containing joint angles of the lower limb at each time step. From the joint angles, the muscle activation levels and muscle forces were calculated using the Static Optimization (SO) tool. SO uses results of the IK to solve the equations of motion for the unknown generalized forces constrained by the force-length-velocity properties while minimizing the cost function [30]. The IK results were filtered using a standard 6 Hz low pass Butterworth filter. Other inputs for SO were external load data, containing ground reaction forces, and a residual and reserve actuators file to compensate for discrepancies between internal and external forces. Output files of the SO were muscle forces and activation levels of each muscle in the lower limb at each time step.

After SO, a joint reaction analysis (JRA) was used to calculate JRFs and moments at the knee joint. The JRA tool calculates joint forces using the loads on the consecutive bodies as input. The resulting forces represent the internal loads in the joint structure. Inputs to the JRA tool are the joint name of interest (left knee: "knee_l"), the body on which the corresponding reaction occurs (tibia expressed as "child"), the frame

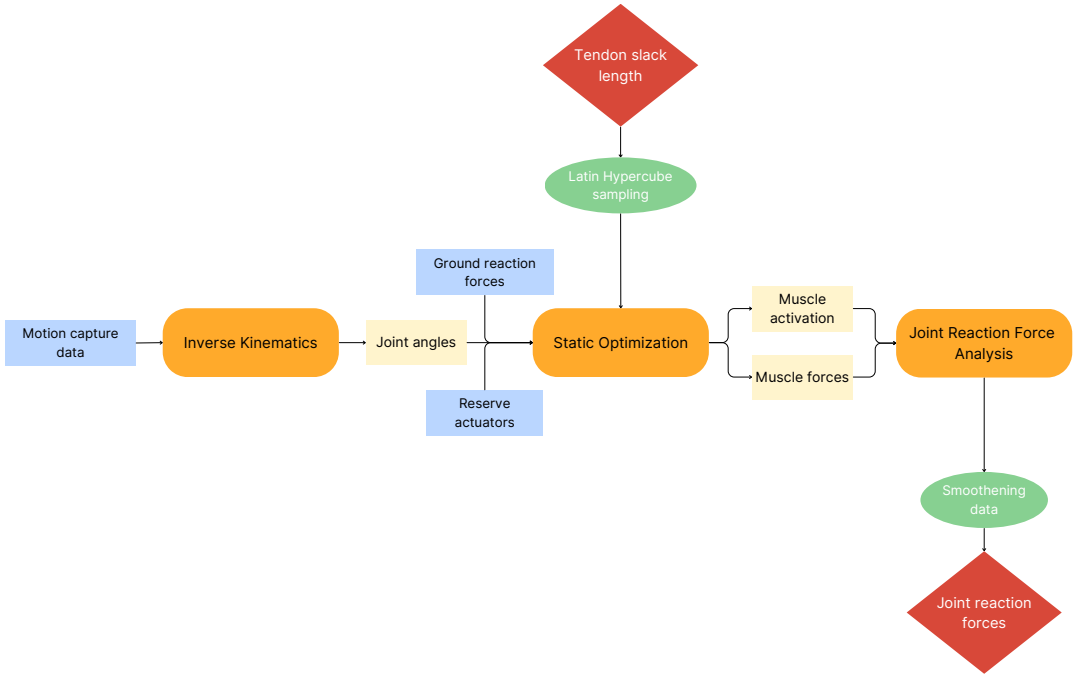

Figure 3: Schematic overview of the established workflow

in which the corresponding reaction is expressed (tibia expressed as "child"). At last, the force file resulting from the SO tool is used as input. The output contains three force (Fx, Fy, Fz) and three moment (Mx, My, Mz) components of tibial reaction load expressed in the tibial reference frame per time step of the gait cycle [31].

2.2 Experimental set up

To understand how uncertainty in TSL affects knee JRF estimations, a twofold research was set up. On the one hand, default TSL values from all muscles in the Gait2392 model were collected [28]. A percentage deviation of +/- 20% was applied on to the values and the resulting range served as the range of input values for one of the experiments [22, 25, 26].

On the other hand, papers on TSL were collected to map the anatomical variation reported in literature. To this end, a literature review using a systemic approach was set up to find articles on muscle parameters [32]. Within this set of articles, studies reporting TSL values were collected as well as references to older papers reporting anatomical measurements and modeling studies to estimate TSL values. Only estimated TSL through modeling studies were included, measured tendon lengths from cadavers were excluded [33]. From the reported TSL values, maximum and minimum values were gathered in a table, see table 2 in Appendix A. The minimum and maximum TSL values resulting from this investigation served as range of input values for the other experiment. Within the consulted studies, only one TSL estimation was found for the external oblique (ext_obl). To improve comparability between the experiments, it was decided to keep the TSL for external oblique in both experiments constant.

To create reference forces, the SO and JRA tool were being run with the nomimal model, with default TSL values. The IK results of the nominal model were used as basis for all simulations. Then, based on the two sets of TSL values, two sensitivity analyses were performed. One sensitivity analysis used reported TSL values as input for the simulations. The other sensitivity analysis used the percentage deviation from the nominal model as input for the simulations. Both experiment consisted of 1000 simulations. To account for uncertainty in TSL values, TSL of all muscles were adjusted in each simulation. The assigned TSL value per muscle per simulation was determined using a Latin Hypercube Sampling (LHS) method [34]. This method provides generation of near-random samples, by dividing the range of TSL values in equal intervals. Each set of TSL values per simulation is created through random allocation of a value within that interval [35]. For each simulation an adjusted MS model was created and the SO and JRA simulation were being run. A convergence analysis was performed to ensure resulting data reached convergence [36] [37].

A python script was used to create the MS models with adjusted TSL values and subsequently run the SO and JRA tool. Running this script was done using the Delftblue High Performance Computer (DHPC). To this end, a python scripting environment for OpenSim on DelftBlue was created. To run the whole workflow, a shell script was used to activate the Opensim scripting environment and run the python script with all MS simulations on DelftBlue. Results were stored on the DHPC and transferred to the local drive for data analysis.

2.3 Data analysis

At first, muscle activation levels in all simulations were evaluated. As maximal neural activation of a muscle is unlikely to occur in reality, it was decided to set a boundary for maximum activation levels. Simulations in which any of the muscles showed activation levels of 0.99 for more than 0.1 seconds were eliminated from further investigation [38] [16]. The assigned TSL values of the failed simulations, the excluded simulations (based on activation levels) and the included simulations were investigated separately.

Raw force data were smoothened using a Gaussian smoothing method. The level of filtering was chosen based on visual inspection of the plotted unfiltered force data from the experiments on anatomical variation, see Appendix B. The first 0.1 seconds were filtered using a sigma of 2.5. The rest of the force data was smoothened with a sigma of 0.7. A transition phase of 10 increments was applied to smoothen out the large difference in sigma values. Data analysis on JRF estimations was performed with the smoothened force data.

For analysis of knee JRFs, force estimations were divided in different periods, corresponding to the different phases of the gait cycle. Within the gait cycle, the stance phase consists of the loading response, midstance, terminal stance and preswing. The swing phase consists of initial swing, mid swing and terminal sing. Variation in JRF estimations was first inspected visually. Then, a 15-85% bound was calculated to identify phases with large variation. Simulations exceeding this bound were deemed to cause large variation. The assigned TSL in simulations exceeding the upper (85%) or lower (15%) bound were examined. Per muscle, the assigned TSLs, in terms of interquartile ranges (IQRs), were plotted against their full TSL range. The IQRs corresponding to simulations resulting in high and low JRFs were compared. Differences were assessed

based on size of IQRs and the location within the full TSL range. Muscles for which the IQRs were clearly off center or different in size were determined to be influential on the extreme JRFs. This analysis was done for the simulations using reported TSL variation and percentage TSL variation. For influential muscles, muscle forces were plotted to investigate relations between assigned TSL, muscle forces and resulting JRFs.

3 Results

3.1 Tendon slack length variation

Figure 4 shows a comparison between the TSL variation reported in literature and the scaled TSL used in the generic MS model including a percentage variation of 20%. The unscaled values from the original Gait2392 model are based on research of Delp et al. (1990) who used anatomical measurements of Wickiewicz et al. (1983), Friedrich & Brand (1990) and Brand et al. (1986) [28, 39, 40, 41]. The scaled values are derived from measurements of the subject used for motion data. Reported anatomical variation in TSL was retrieved from papers reporting TSL values based on anatomical measurements combined with modeling studies. An overview of the maximum and minimum TSL values can be found in Appendix A. The TSL estimations are taken directly from earlier research and could not be normalized to other muscle parameters or the subjects measurements.

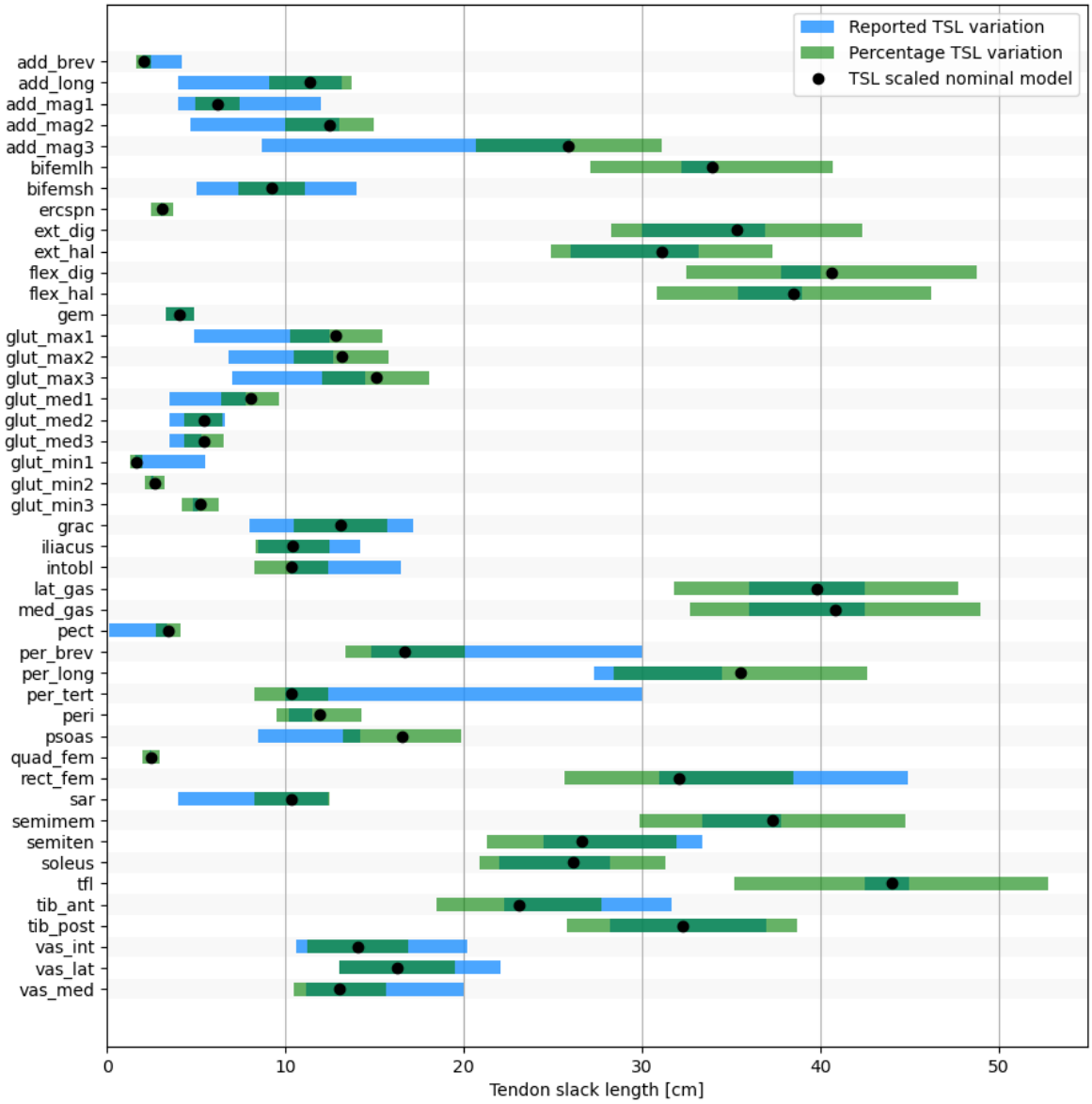

Figure 4: Range of TSL values based on reported variation in literature (blue) and percentage variation of 20% (green) applied on the default TSL values of the nominal model (black).

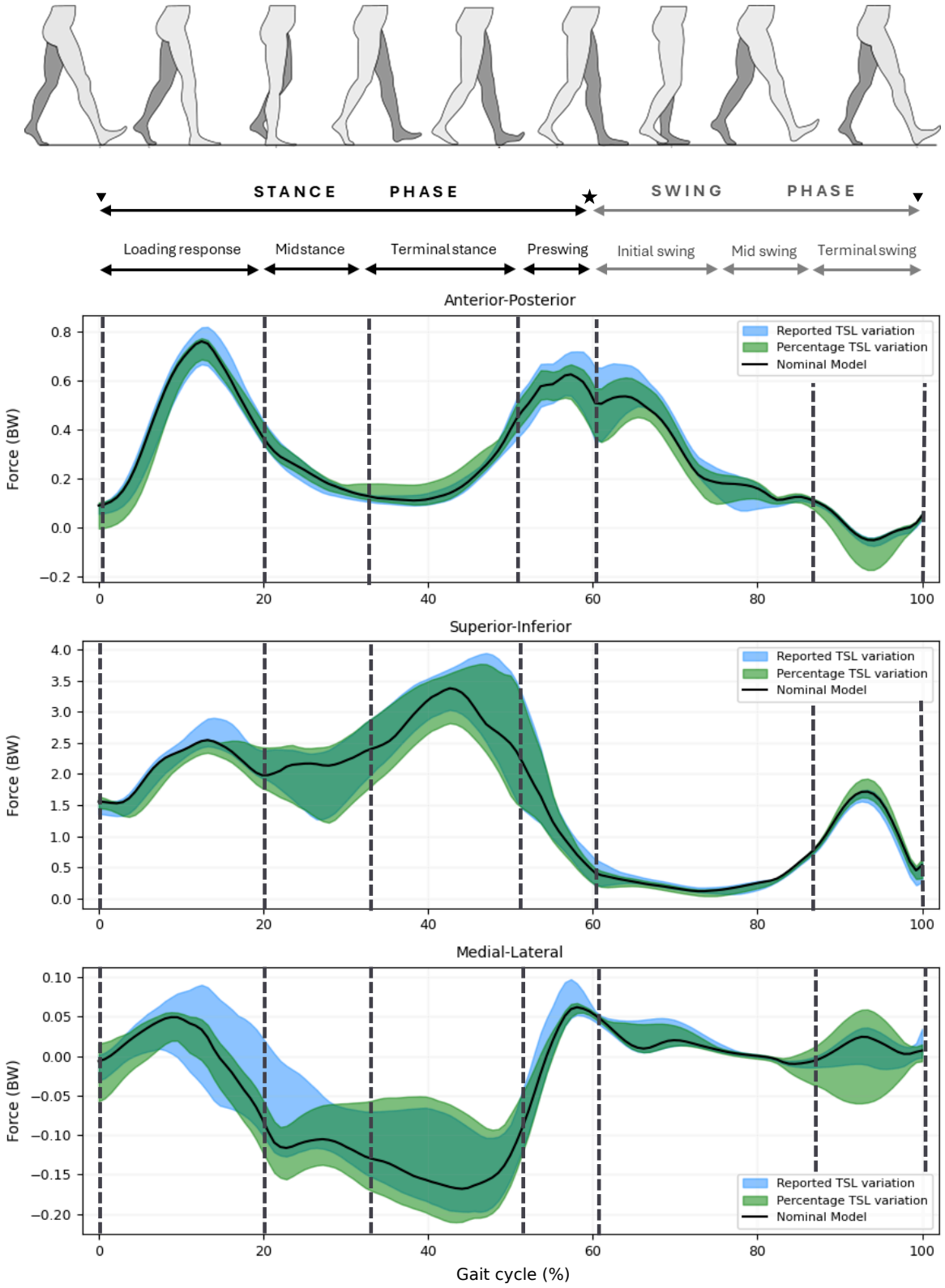

Figure 5: JRF estimations resulting from simulations using reported TSL variation (blue) and percentage TSL variation (green). JRF estimations of the nominal are plotted in black. For reference the difference phases of the gait cycle are displayed above the plots [42]. The triangles (▼) indicate the start of the heel strike and the star (★) indicates the moment of toe-off.

3.2 Joint reaction forces

3.2.1 General findings

The SO failed for 33 simulations when using reported TSL variation and 24 simulations when using percentage TSL variation (Appendix C). Within the simulations that ran successfully the SO was not able to calculate muscle forces for all muscles. In the simulations using reported TSL variation, the pre-set boudaries for muscle activation were exceeded in 31 simulations. In the simulations using percentage TSL variation, 418 simulations exceeded muscle activation levels. It was found that within these simulations, the assigned TSL values for soleus smaller than 21.7 cm and larger than 29.3 cm resulted in activation levels that exceeded pre-set boundaries, i.e. higher than 0.99 for 0.1 seconds.

Variation in JRF estimations was the largest during the stance phase, see figure 5. Maximum calculated variation over all simulations was 0.27 x BW in AP direction, 2 x BW in SI direction and 0.13 x BW in ML direction. When considering peak forces in the loading response, the maximum reached JRFs for simulations with reported TSL variation were higher compared to simulations with percentage variation: 0.25 x BW in AP, 0.4 x BW in SI, and 0.04 x BW in ML direction. In the terminal stance and pre-swing, highest JRFs were also reached through simulations with reported TSL variation: 0.25 x BW in the SI direction in the terminal stance phase, and 0.08 x BW in AP 0.04 x BW in ML direction in the pre-swing phase. Contrastingly, percentage TSL variation led to increased JRF estimation of 0.02 x BW in ML direction during the terminal stance.

Generally the JRF estimations of the nominal model were on the upper bound of the simulations resulting from percentage TSL variation. Apart from magnitude of JRFs and the sensitivity to uncertainty in TSL, the timing of JRF estimations differed slightly between the two approaches. In SI direction, some of the simulations with reported TSL variation resulted in delayed peak force in the terminal stance phase. Similarly, in ML direction reported TSL variation resulted in delayed peak forces during loading response.

3.2.2 Anterior-posterior

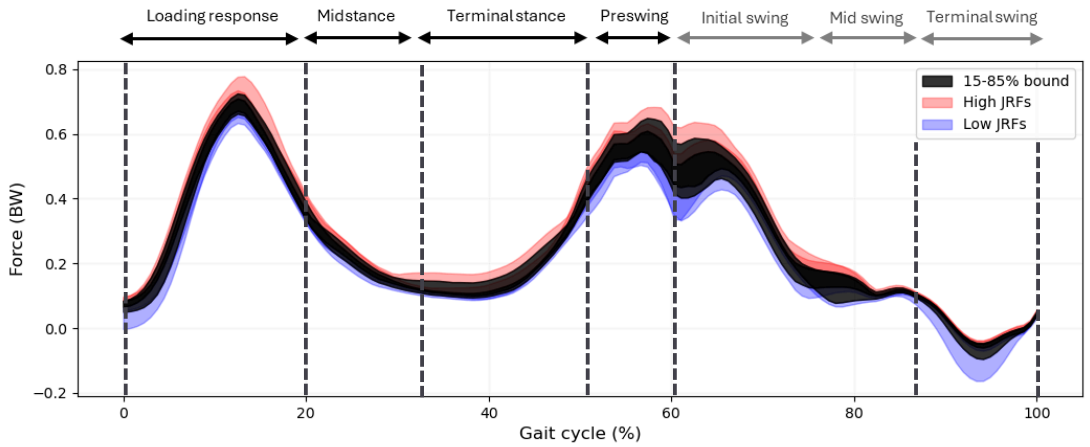

Figure 6: Estimated JRFs in anterior-posterior direction, with 15-85% bound (black) and high (red) en low JRFs (blue).

Plotting the assigned TSL values that led to high and low JRFs in AP direction (fig. 6), TSL of rectus femoris (rect_fem), biceps femoris long head (bifemlh), semimembranosus (semimem) and psoas showed most differing TSL values, see figure 7. Within the range of reported TSL variation, low TSL of psoas led to decreased muscle force and to increased JRFs, see figure 8a. When comparing the reported TSL variation with the percentage TSL variation of psoas, decreased TSL led to decreased MF and increased knee JRFs. Even though the assigned TSL values for biceps femoris long head and semimembranosus resulting in high and low JRFs were also different, muscle force of biceps femoris long head and semimemembranosus were negligible during the pre-swing phase. The IQRs of assigned TSL values of rectus femoris were different for high and low JRFs. Nevertheless, resulting muscle forces showed no clear differences, see figure 8b.

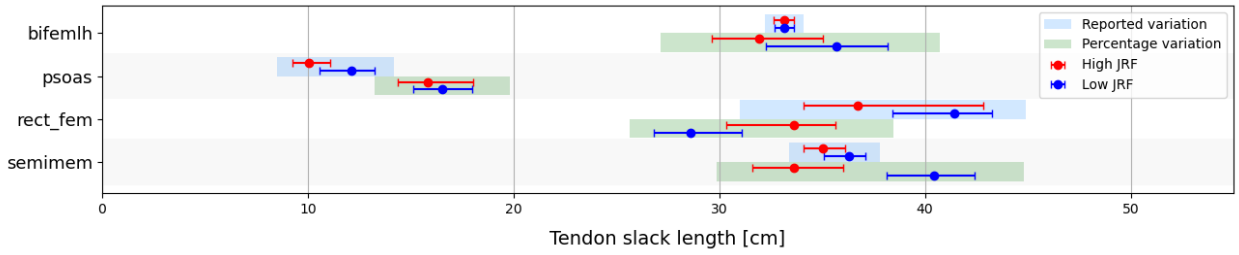

Figure 7: Assigned TSL values around toe-off in AP direction for high (red) and low (blue) JRF estimations. TSL of simulations present in the red or blue area (fig. 6) were investigated. Assigned TSL for these
:h

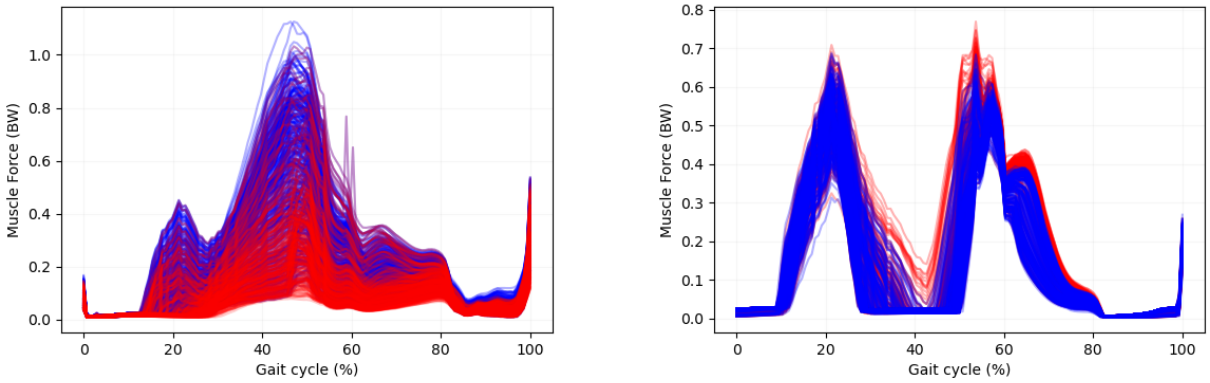

(a) Psoas (reported TSL variation)

(b) Rectus femoris (percentage TSL variation

Figure 8: Muscles forces for simulations resulting in high (red) and low (blue) JRFS around toe-off (55-70%) in AP direction

3.2.3 Superior-inferior

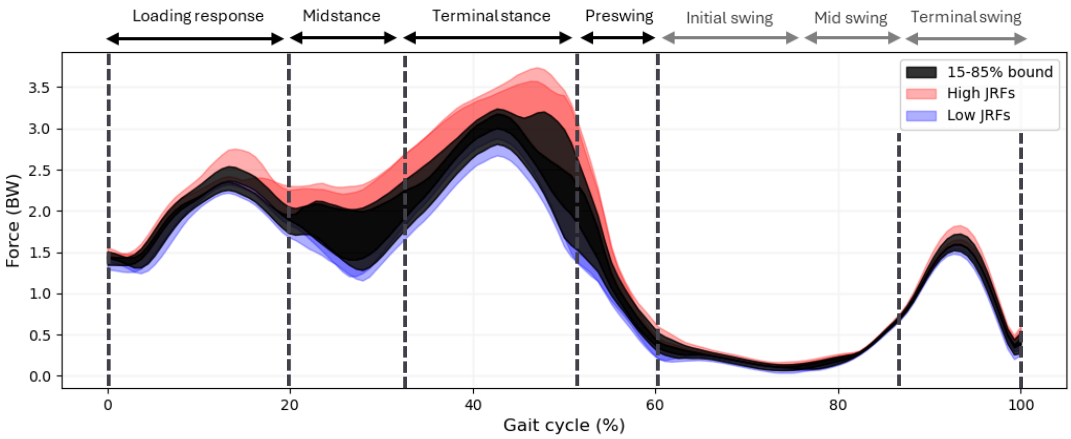

Figure 9: Estimated JRFs in superior-inferior direction, with 15-85% bound (black) and high (red) en low JRFs (blue).

In SI direction, muscles showing most differing TSLs for high and low JRFs were the same for midstance and terminal stance (fig. 10). The IQRs of assigned TSL values for gastrocnemius medialis in simulations resulting in higher JRFs were very small. Contrastingly, for simulations using percentage variation, the IQR of assigned TSL was very large. The assigned TSL values for simulations resulting in lower JRFs were either lower than 0.38 cm or higher than 0.43 cm. TSLs between 3.9 and 4.3 cm resulted in higher muscle forces (fig. 11a) and thus higher JRFs. A similar relation was found for gastrocnemius medialis in simulations using reported TSL variation. For rectus femoris, lower TSL led to increased muscle force and to increased JRFs.

Differences in assigned TSLs for soleus were not large, but muscle forces indicated that the small difference in TSL did lead to difference in muscle force of 0.8 x BW, see figure 11b.

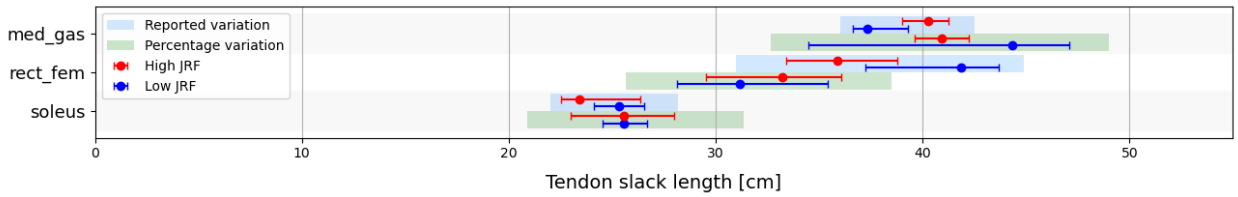

Figure 10: Assigned TSL values during midstance in SI direction for high (red) and low (blue) JRF estimations. TSL of simulations present in the red or blue area (fig 9) were investigated. Assigned TSL for these simulations were calculated for all muscles. Muscles with the largest difference in assigned TSL are displayed.

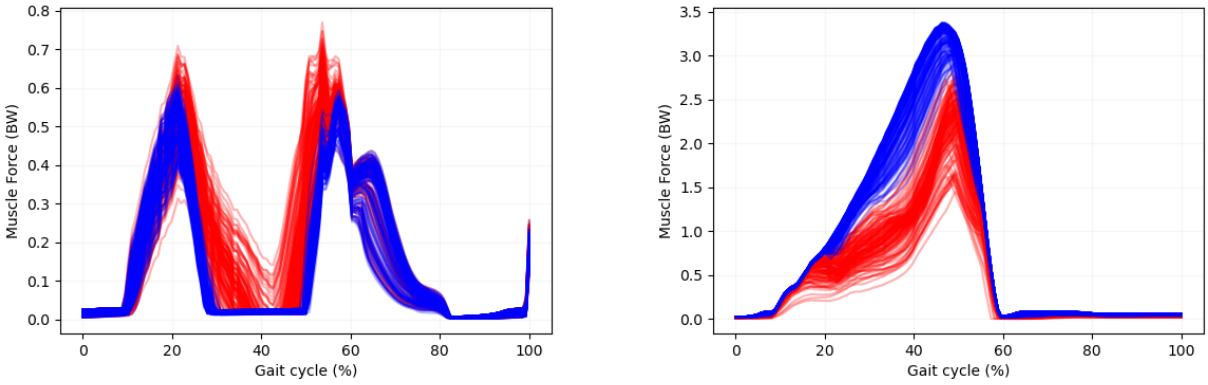

(a) Rectus femoris

(b) Soleus

Figure 11: Muscle forces for simulations reaching high (blue) and low (red) superior-inferior JRFs during midstance (20-35%) using reported TSL variation

3.2.4 Medial-lateral

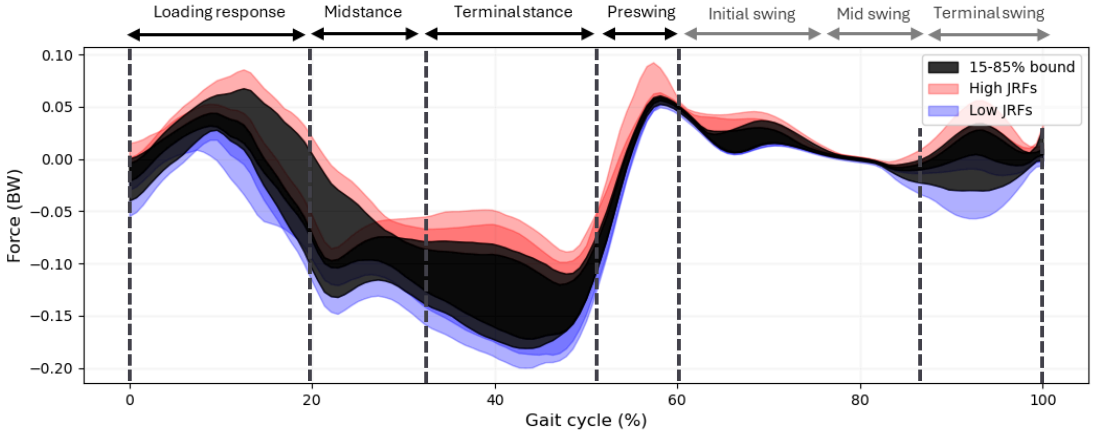

Figure 12: Estimated JRFs in mediolateral direction, with 15-85% bound (black) and high (red) en low JRFs (blue).

Loading response (0-20%)
In ML direction, variation JRF estimations were mainly sensitive to TSL variation during loading response, terminal stance and pre-swing (fig. 12). Gluteus maximus (middle part) (glut_max2), gluteus medius anterior (glut_med1), rectus femoris and vastus lateralis (vas_lat) showed most differing TSL values for high and low JRFS during the loading response (fig. 13). Plotting muscle forces for the gluteus medius (anterior side)

(glut_med1) indicated that low TSL values led to decreased muscle forces and increased JRFs, see figure 14a. Within the range of percentage TSL variation, high TSL for gluteus maximus 2 led to decreased muscle forces and higher knee JRFs. Muscle forces of gluteus medius anterior generated by the two experiments were found to differ to similar extent as shown in figure 14a. Results on TSL and muscle forces of rectus femoris during the loading response indicated that higher TSL led to decreased muscle force and increased JRFs. This applied to assigned TSL values within a range, but also when comparing the two experiments. Vastus lateralis (vas_lat) showed lower TSL resulted in increased MF and higher JRFs (fig. 14b).

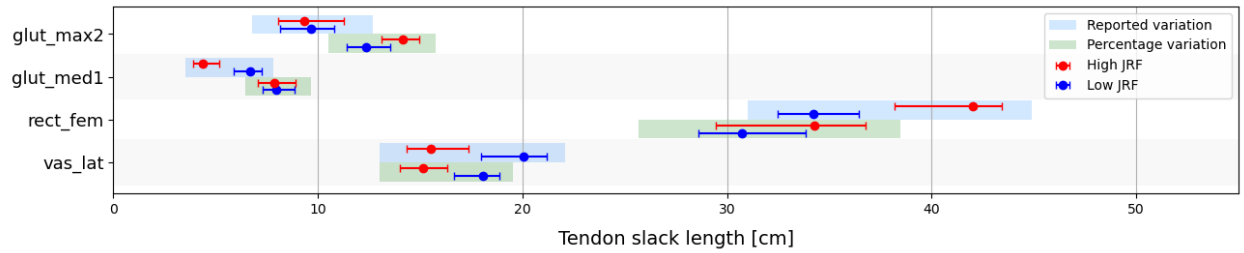

Figure 13: Assigned TSL values during loading response in ML direction for high (red) and low (blue) JRF estimations. TSL of simulations present in the red or blue area (fig. 12) were investigated. Assigned TSL for these simulations were calculated for all muscles. Muscles with the largest difference in assigned TSL are displayed

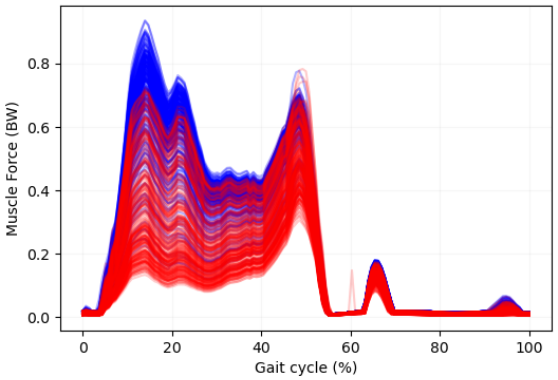

(a) Gluteus medius (anterior)

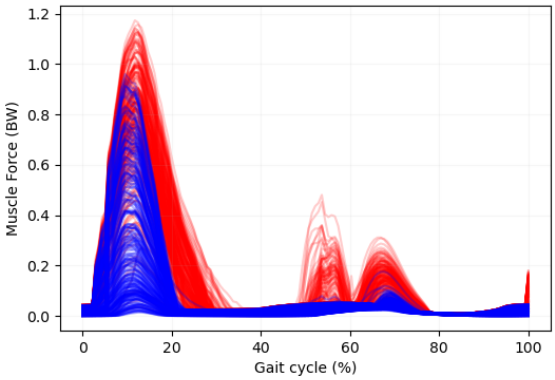

(b) Vastus lateralis

Figure 14: Muscle forces for simulations reaching high (red) and low (blue) JRFs in the loading response (0-20%)

Terminal stance (35-55%)

The pattern of JRFs for both experiments is similar during the the terminal stance. Muscles that were assigned most differing TSL values for high and low JRFs were gastrocnemius lateralis (gas_lat) and med_gas, see figure 15. It is important to note that during terminal stance in ML direction, the negative JRFs are directed to the lateral side of the knee. Low JRF estimations, displayed in blue, are thus not necessarily low forces but rather directed in lateral direction while high (positive) JRF are directed in a (relatively) more medial direction. Figure 15, 16b and 16a show that lat_gas and med_gas were found to have an opposite relation with respect to the mediolateral forces in the knee. For simulations in which JRFs were high in lateral direction, the IQR for med_gas was between 0.4 and 0.42 cm and assigned TSL for lat_gas were on the extreme lower or higher side of the range. For simulation in which JRFs were more directed to the medial side, the IQR of lat_gas was between 0.38 and 0.42 cm and the assigned TSL values were lower than 0.38 cm or higher than 0.46 cm.

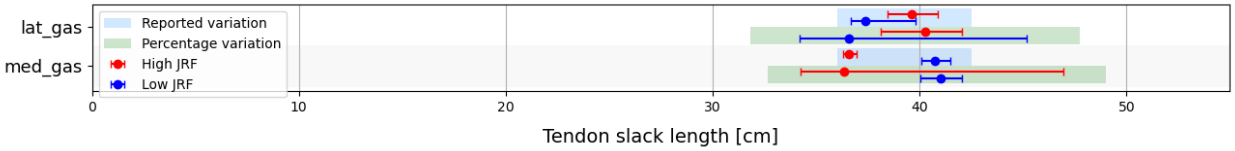

Figure 15: Assigned TSL values during loading response in ML direction for high (red) and low (blue) JRF estimations. TSL of simulations present in the red or blue area (fig. 12) were investigated. Assigned TSL for these simulations were calculated for all muscles. Muscles with the largest difference in assigned TSL are displayed

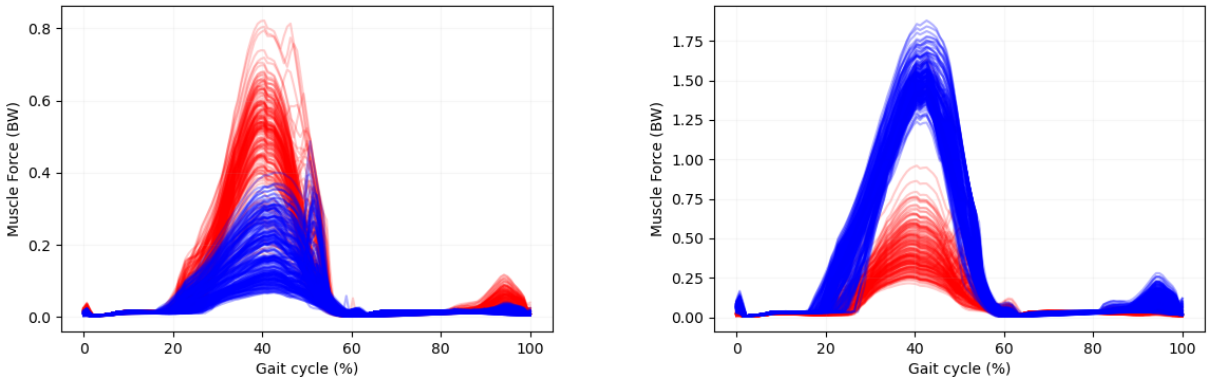

(a) Gastrocnemius lateralis

(b) Gastrocnemius medialis

Figure 16: Muscle forces in ML direction from simulations reaching high (red) and low (blue) JRFs using percentage TSL variation in the terminal stance (30-50%)

3.3 Comparison

To summarize, table 1 list the muscles for which the TSLs were most different for high and low JRFs estimations. Differences with regard to influential muscles were limited. The main distinction can be found within the different phases within the directions.

Table 1: Muscles with most different assigned TSL for high and low JRF estimations.

	Stance Phase		**Swing Phase**	
	Reported variation	**Percentage variation**	**Reported var.**	**Percentage var.**
AP	Glut_med1, Vas_lat	Glut_max2, Vas_lat	Rect_fem, psoas	Rect_fem, Semimem, Bifemlh
SI	Glut_med1, Med_gas, Rect_fem, Psoas	Glut_max2, Med_gas, Lat_gas, Soleus, Psoas		
ML	Glut_med1, Rect_fem, Vas_lat, Lat_gas, Med_gas	Glut_max2, Rect_fem, Lat_gas, Med_gas, Vas_lat	Semimem, Vas_lat, Rect_fem	Semimem, Lat_gas, Med_gas, Rect_fem

Bifemlh – Biceps Femoris Long Head, *Glut_max2* – Gluteus Maximus (middle part), *Glut_med1* – Gluteus Medius anterior, *Lat_gas* – Lateral Gastrocnemius, *Med_gas* – Medial Gastrocnemius, *Rect_fem* – Rectus Femoris, *Semimem* – Semimembranosus, *Vas_lat* – Vastus Lateralis.

4 Discussion

4.1 General findings

This thesis investigated how uncertainty in TSL of lower limb muscles affect knee JRF estimations in gait analysis. Uncertainty in TSL was approached in a two-fold way: reported TSL values in literature were collected to gain insight in the anatomical variation reported in literature. The other approach used the default TSL from a generic MS model and applied a percentage perturbation of 20% to create a range of TSL variation. The sets of TSL values formed the basis for two sensitivity analyses using MSM to investigate resulting variation in JRF estimations.

Results of the literature review on reported TSL revealed that data on muscle parameters for some muscles is limited. As a result, the TSL range for some muscles was very small and the differences in assigned TSL per simulations were hard to visualize. Consequently, their influence on JRF estimations remained unclear. For the approach of percentage TSL variation, the ranges for TSL were proportional to the default TSL in the nominal model. As a result, TSL ranges were larger for higher default TSL. Anatomical variation reported in literature does not confirm this relation. The comparison in figure 4 shows that TSL ranges defined by percentage variation were larger when TSL exceeded 30 cm and smaller with TSL lower than 20 cm. It can be concluded that both approaches have their limitations and the present study is necessary to assess the effect of these limitations.

Results on muscle activation levels showed that extreme variations in TSL of the soleus led to excessive activation. In the nominal model, soleus activation was the highest, and extreme perturbations of the default TSL value resulted in unphysiological activation levels [16, 38]. Veen et al. (2019) investigated the effect of muscle recruitment on joint loading in the lower limb and found that increased soleus activation led to decreased knee contact forces, and vice versa [43]. This highlights the importance of carefully handling soleus TSL when aiming for patient-specific MSM outcomes.

Results of the nominal model and the simulations using percentage TSL variation indicate that the relation between TSL and resulting JRFs is rather complex. Even though the TSL values in the nominal model are the exact median of the percentage TSL variation ranges, the JRFs were on the upper or lower bound of all simulations with percentage TSL variation. It can be concluded that mean TSL do not necessarily lead to average JRF estimations.

4.2 Joint reaction forces

The overall variation in JRFs estimations as a result of uncertainty in TSL aligns with the range reported in the literature. Axial joint forces during gait typically range from 2 to 3.5 $\times$ BW in in-vivo estimations [44, 45, 46]. In-vitro measurements extend this range up to 5 $\times$ BW, as reported by Morrison (1970) and Taylor et al. (2004) [47, 48]. Similarly, AP shear forces during walking fall between 0.3–0.6 $\times$ BW in in-vivo studies [45, 48]. According to Kutzner et al. (2010), ML shear forces vary between $-0.18 \times$ BW and $0.16 \times$ BW [49]. These findings suggest that the variation in JRFs due to uncertainty in TSL is comparable to the variability reported in the literature. However, force estimations in previous studies are often derived from modeling approaches using multiple subjects. This highlights the inherent challenge of personalized MSM for clinical applications, because results in this study indicate that uncertainties in TSL can influence MSM outcomes to a similar extent as variations between subjects.

Results on muscle specific TSL showed some interesting relations. Assigned TSL in AP direction indicate that psoas, rectus femoris, semimembranosus and biceps femoris long head are most important to take into consideration when aiming for accurate force estimation in AP direction. Results on psoas showed that increased JRFs were obtained with lower TSL and lower muscle forces. Results in the loading response of the gait cycle also idicated that hip crossing muscles are influential in JRF estimations. Reported TSL variation showed that TSL of gluteus medius anterior was influential in JRFs whereas percentage variation showed that gluteus maximus is influential in JRFs. Related muscle forces confirm the findings of Bicer et al. (2022) who stated that decreased muscle forces in hip crossing muscles lead to increased knee JRFs, due to compensatory behavior of knee crossing muscles [50]. Muscle forces of semimembranosus and biceps femoris were negligible in around toe-off. This indicates that even though different TSLs were assigned to high en low JRFs, no clear relation can be found between the TSL of the hamstring muscles and the JRF estimations. Muscle forces of rectus femoris show that even though different TSLs were assigned to simulation resulting in high and low JRFs, muscle forces for those simulations were not clearly different. Carbone et al. (2016) describes this with the concept of overall sensitivity. They investigated the effect of muscle parameters on muscle forces of surrounding muscles and found that rectus femoris is one of the muscles that is most depending on TSL of surrounding muscles [22]. This is also reflected in the results in SI direction, where relatively small differences

in TSL of soleus did result in obvious differences in muscle forces. Altogether it can be concluded that even though for some muscles different TSL were found for high and low JRFs, the link between TSL, muscle force and JRFs is far from straight . As a result, muscle specific causes for the increased JRF estimations in SI direction were hard to find. Assigned TSL for high and low JRF estimations were not distinct. Results of JRF estimations in ML direction indicate that accurate estimation of TSL of gastrocnemius muscles is important. Increased muscle force in gastrocnemius resulted in increased JRFs in lateral direction and vice versa. The gastrocnemius muscles are attached to the tibial condyles, situated between the tendons of the biceps and semimembranosus. Consequently, muscle forces generated by gastrocnemius medialis has a slight lateral component whereas gastrocnemius lateralis has a slight medial force components. Uncertainty in TSL of gastrocnemius can thus severely influence force distributions along the mediolateral axis. Even though JRF estimations in ML direction were relatively small compared to the other directions, variation in this direction should be carefully considered for KOA research. The results showed a relatively large variation in force distribution along the mediolateral axis as a result of uncertainty in TSL. Accurate estimation of mediolateral forces are crucial to assess gait patterns and subsequent knee loading. Abnormal loading due to knee malalignment is one of the main causes of KOA development and should thus be noticed when performing patient-specific MSM [51, 52]. Force distribution along this axis could be an indicator of increased shear forces, which is considered a risk for development of KOA [51, 53].

4.3 Comparison

Comparion of the two experiments indicated that despite the different used TSL ranges, variation in JRF estimations were comparable. Additionally, muscles that were found to be influential in JRF estimations were similar. Only the hip muscle, soleus and bifemlh were differing between the two experiments. Overall results with respect to influential muscles are in line with other studies [22, 23, 54].

4.4 Limitations

The conducted research has some limitations. When creating the sets of TSL ranges, TSLs found in literature could not be normalized to measurements of the subject. Datasets on muscle parameters present in literature are the product of a few cadaveric measurements combined with modeling studies [39, 40, 55]. Datasets resulting from modeling studies have been improved over the past decades and consequently, references on original anatomical measurements as well as information of the subjects providing experimental data are not always present. Thus, including reported anatomical variation in literature can be considered as an alternative approach within sensitivity analyses on muscle parameters. However, the found TSL range should be handled with care and cannot be considered as the true variation present in human beings. This is also reflected in the fact that data on some muscles were very limited. As a result, the range for those muscles were very small and possible affects on JRFs were hard to investigate. The reason for limited data can be traced down to progress of MS development over the past decades. Early cadaveric studies focused only on muscle groups [56, 57], whereas later studies focused on all separate muscles. Moreover, with the development of increasingly detailed and complex MS models, some muscles, like glutei muscles, are currently represented by multiple muscle muscletendon actuator requiring more muscle parameter measurements in each separate muscle parts [9, 33]. Thus, comparison between older and more recent anatomical studies was challenging because of their different levels of detail. The fact that TSL values of certain muscle are estimated more often, and potentially more accurately than others, could influence MF and JRF estimation.

A second limitation is the investigation of one single muscle parameters. Even though TSL is found to be most influential in muscle force generation, muscles functionality is determined by the interaction of all mechanical parameters [16]. Changing only one parameter, while keeping the others constant, does not capture the interdependent relation between the muscle parameters. Moreover, the found reported TSL variations are often based on assumptions with respect to, for instance, OFL [21, 58, 59]. Only adjusting TSL could have led to unrealistic ratios between the two mechanical parameters. The relation between fiber and tendon length was investigated by Mörl et al. (2015). They found that extreme ratios resulted in excessive force generation and changed contraction velocity [60]. Since contraction velocity is determined by activation dynamics, it could be argued that both JRFs estimations and muscle activation could have been influenced by extreme TSL.

Additionally, since all TSLs were adjusted simultaneously, certain combinations of TSL were potentially not realistic in terms of the subjects measurements. This was confirmed by the results of the SO in which for some muscles, muscle forces could not be calculated. These muscles were not taken into consideration for later consulted muscle forces resulting from TSL variation. Combinations of extreme TSL might have led to excessive muscle activation and extreme JRF estimations. At last, due to the excessive soleus activation levels,

nearly half of the simulations with TSL variation had to be excluded. Consequently, results on percentage-based TSL variations were are based on only half the amount of data compared to simulations with reported TSL values.

Another limitation of this study is the use of a single DoF knee model to estimate joint reaction forces (JRFs). While this simplified approach allows for a more manageable and computationally efficient analysis, it does not fully capture the complex, multi-dimensional dynamics of the knee joint. The knee operates across multiple degrees of freedom, and a single-DOF model may miss key contributions from movements like rotation or lateral translations. As a result, this limitation could impact the accuracy and clinical relevance of the JRF estimations. Additionally, the subject whose experimental data was used had a history of ACLR. It is well established that knee joint loading increases after ACLR due to altered mechanics [61]. Since this model does not account for the ligaments in the knee, the changes in joint loading following ACLR trauma cannot be accurately represented.

4.5 Further research

4.5.1 Musculoskeletal modeling

Uncertainty in muscle parameter estimation is hard eliminate. Further research should focus on developing measuring techniques to estimate muscle parameters in-vivo. Similarly, a more extensive and complete database of measured muscle properties should be created, since Yamaguchi, et al. (1998) was the last one collecting different datasets. The past decades the same datasets have been iteratively re-used and improved, but initial measurements are all stemming from a few cadavers [21]. More cadaver measurements will contribute to a better representative of anatomical variation in research. Together with improved in-vivo measuring techniques, data on anatomical variation could aid to develop personalized MSM modeling.

Found JRFs indicate that uncertainty in TSL affect JRF estimations mostly during the stance phase. For further research, observing the stance phase alone can be considered sufficient. Largest absolute variation in JRFs was found in SI direction and largest relative variation in ML direction. For research in KOA, accurate estimation of JRFS in those direction should thus be the main focus. Additionally when estimating JRFs as accurate as possible, TSL of lateral gastrocnemius, medial gastrocnemius, rectus femoris, vastus lateralis and psoas should considered specifically. Even though in-vivo estimation is challenging, TSL used in the MS should be estimated as accurate as possible by considering other parameters that are more easy measurable [18, 62]. Scaling through optimization techniques could also aid to make better estimations in muscle parameters [63, 64].

4.5.2 Finite element modeling

This research was limited to investigation of knee JRF. To understand how patient-specific muscle properties contribute to the development of KOA, it is crucial to link the insights of knee JRF to tibiofemoral AC response. Finite elment modeling (FEM) could aid to gain insights in AC degeneration as a result of variation in JRF estimations. For instance, JRFs of a simulation with increased forces in medial direction could be compared with a simulation with increased forces in lateral direction. Resulting tissue response could indicate how AC is affected by force distribution patterns from different TSLs. In earlier stages of this research, an experiment was set to up to use resulting JRFs from the MSM experiments as input for an FE knee model. Specifications of the FE knee model and the experimental set up can be found in Appendix D. As input for the FE model, two simulations were selected with deviating force estimations up to 1 x BW in SI direction. Calculated stress responses in the AC resulting from this JRF variation were negligible. Ligament stresses were found to be 3 orders of magnitude larger than calculated stress in the AC. According to Shelburne et al. (2005) ligament forces range up to 0.45 x BW [65]. Additionally, stress in the ligaments were both negative and positive, indicating non-physiological behavior. Altogether, the results of the FE knee model were deemed unreliable for drawing meaningful conclusions. Further research could improve the FE model by representing ligaments as non-linear springs while ensuring simulation stability. If the model can reliably capture AC stress responses based on JRF estimations between 2 x 4 times BW, future studies can explore the impact of TSL on AC stress response.

5 Conclusion

This research investigated the effect of uncertainty in TSL on JRF estimations in gait analysis. This was done by conducting two sensitivity analyses using MSM. One experiment used anatomical variation reported in literature as input values. The other approach used a percentage variation from the nominal TSL values in a generic MS model. Maximum calculated variation over all simulations was 0.27 x BW in AP direction, 2 x BW in SI direction and 0.13 x BW in ML direction. Maximum reached JRFs for simulations with reported TSL variation were higher compared to simulations with percentage variation: 0.25 x BW, 0.4 x BW, and 0.04 x BW for AP, SI and ML direction respectively. In the terminal stance, highest JRFs were also reached through simulations with reported TSL variation: also resulted in greater JRFs in the SI (0.25 x BW) direction in the terminal stance phase, and in AP (0.08 x BW) and ML (0.04 x BW) direction in the pre-swing phase. Contrastingly, percentage TSL variation led to increased JRF estimation of 0.02 x BW in ML direction during the terminal stance. Muscles that were found to be influential in JRF estimations despite of the used TSL range were both gastrocnemius muscles, rectus femoris, vastus lateralis and psoas. Gastrocnemius muscles were found to be mostly influential in ML direction and it was concluded that for KOA, these results should be carefully considered. The study highlights that TSL uncertainty can substantially impact knee JRF estimations and should be carefully considered when developing patient-specific MSM for clinical applications. Future research should aim to investigate how variation in JRF estimations affect stress response in the AC. This will aid the development of personalized MSM for KOA purposes.

References

[1] W. H. O. WHO, "Osteoarthritis," World Health Organization: WHO, 2023.

[2] T. Neogi and Y. Zhang, "Epidemiology of osteoarthritis," *Rheumatic Diseases Clinics of North America*, vol. 39, no. 1, p. 1–19, 2013.

[3] F. Guilak, "Biomechanical factors in osteoarthritis," *Baillière's best practice and research in clinical rheumatology/Bailliere's best practice research. Clinical rheumatology*, vol. 25, no. 6, pp. 815–823, 12 2011.

[4] J. Kellgren and J. S. Lawrence, "Radiological assessment of osteo-arthrosis," *Annals of the Rheumatic Diseases*, vol. 16, no. 4, p. 494–502, 1957.

[5] T. P. Andriacchi, A. Mündermann, R. L. Smith, E. J. Alexander, C. O. Dyrby, and S. Koo, "A framework for the in vivo pathomechanics of osteoarthritis at the knee," *Annals of Biomedical Engineering*, vol. 32, no. 3, p. 447–457, 2004.

[6] M. Booij, R. Richards, J. Harlaar, and J. Van Den Noort, "Effect of walking with a modified gait on activation patterns of the knee spanning muscles in people with medial knee osteoarthritis," *The Knee*, vol. 27, no. 1, pp. 198–206, 12 2019. [Online]. Available: https://doi.org/10.1016/j.knee.2019.10.006

[7] H. R. B. A. Razak, J. P. Campos, R. S. Khakha, A. J. Wilson, and R. J. Van Heerwaarden, "Role of joint distraction in osteoarthritis of the knee: Basic science, principles and outcomes," *Journal of Clinical Orthopaedics and Trauma*, vol. 24, p. 101723, 12 2021. [Online]. Available: https://doi.org/10.1016/j.jcot.2021.101723

[8] V. Turppo, R. Sund, J. Huopio, H. Kröger, and J. Sirola, "Physical capability after total joint arthroplasty: long-term population-based follow-up study of 6,462 women," *Acta Orthopaedica*, vol. 92, no. 5, pp. 551–556, 5 2021.

[9] S. L. Delp, F. C. Anderson, A. S. Arnold, P. Loan, A. Habib, C. T. John, E. Guendelman, and D. G. Thelen, "OpenSiM: Open-Source software to create and analyze dynamic simulations of movement," *IEEE transactions on bio-medical engineering/IEEE transactions on biomedical engineering*, vol. 54, no. 11, pp. 1940–1950, 11 2007.

[10] S. S. Farshidfar, J. Cadman, D. Deng, R. Appleyard, and D. Dabirrahmani, "The effect of modelling parameters in the development and validation of knee joint models on ligament mechanics: A systematic review," *PloS One*, vol. 17, no. 1, p. e0262684, 2022.

[11] A. D. Sylvester, S. G. Lautzenheiser, and P. A. Kramer, "A review of musculoskeletal modelling of human locomotion," *Interface Focus*, vol. 11, no. 5, p. 20200060, 2021.

[12] L. Sharma, J. S. Chmiel, O. Almagor, D. Felson, A. Guermazi, F. Roemer, C. E. Lewis, N. Segal, J. Torner, T. D. V. Cooke, J. Hietpas, J. Lynch, and M. Nevitt, "The role of varus and valgus alignment in the initial development of knee cartilage damage by MRI: the MOST study," *Annals of the Rheumatic Diseases*, vol. 72, no. 2, pp. 235–240, 5 2012.

[13] D. Felson, "Osteoarthritis as a disease of mechanics," *Osteoarthritis and Cartilage*, vol. 21, no. 1, pp. 10–15, 10 2012.

[14] T. Neogi, M. A. Bowes, J. Niu, K. M. De Souza, G. R. Vincent, J. Goggins, Y. Zhang, and D. T. Felson, "Magnetic resonance Imaging–Based Three-Dimensional bone shape of the knee predicts onset of knee osteoarthritis: data from the Osteoarthritis Initiative," *Arthritis Rheumatism*, vol. 65, no. 8, pp. 2048–2058, 7 2013. [Online]. Available: https://doi.org/10.1002/art.37987

[15] M. Avci and N. Kozaci, "Comparison of X-Ray imaging and computed tomography scan in the evaluation of knee trauma," *Medicina*, vol. 55, no. 10, p. 623, 9 2019.

[16] T. S. Buchanan, D. G. Lloyd, K. Manal, and T. F. Besier, "Neuromusculoskeletal Modeling: Estimation of Muscle Forces and Joint Moments and Movements from Measurements of Neural Command," *Journal of Applied Biomechanics*, vol. 20, no. 4, pp. 367–395, 11 2004.

[17] F. Michaud, M. Lamas, U. Lugrís, and J. Cuadrado, "A fair and EMG-validated comparison of recruitment criteria, musculotendon models and muscle coordination strategies, for the inverse-dynamics based optimization of muscle forces during gait," *Journal of neuroengineering and rehabilitation*, vol. 18, no. 1, 1 2021.

[18] K. Manal and T. S. Buchanan, "Subject-Specific Estimates of tendon slack Length: a Numerical Method," *Journal of Applied Biomechanics*, vol. 20, no. 2, pp. 195–203, 5 2004.

[19] L. Modenese, E. Ceseracciu, M. Reggiani, and D. G. Lloyd, "Estimation of musculotendon parameters for scaled and subject specific musculoskeletal models using an optimization technique," *Journal of Biomechanics*, vol. 49, no. 2, pp. 141–148, 11 2015.

[20] G. T. Yamaguchi and F. E. Zajac, "A planar model of the knee joint to characterize the knee extensor mechanism," *Journal of Biomechanics*, vol. 22, no. 1, pp. 1–10, 1 1989. [Online]. Available: https://doi.org/10.1016/0021-9290(89)90179-6

[21] Z. Chen and D. W. Franklin, "Musculotendon parameters in lower limb models: simplifications, uncertainties, and muscle force estimation sensitivity," *Annals of Biomedical Engineering*, vol. 51, no. 6, pp. 1147–1164, 3 2023. [Online]. Available: https://doi.org/10.1007/s10439-023-03166-5

[22] V. Carbone, M. M. van der Krogt, H. F. J. M. Koopman, and N. Verdonschot, "Sensitivity of subject-specific models to hill muscle-tendon model parameters in simulations of gait," *Journal of Biomechanics*, vol. 49, no. 9, pp. 1953–1960, 2016.

[23] F. De Groote, A. Van Campen, I. Jonkers, and J. De Schutter, "Sensitivity of dynamic simulations of gait and dynamometer experiments to hill muscle model parameters of knee flexors and extensors," *J Biomech*, vol. 43, no. 10, pp. 1876–83, 2010.

[24] C. A. Myers, P. J. Laz, K. B. Shelburne, and B. S. Davidson, "A probabilistic approach to quantify the impact of uncertainty propagation in musculoskeletal simulations," *Annals of biomedical engineering*, vol. 43, no. 5, pp. 1098–1111, 11 2014.

[25] C. Redl, M. Gfoehler, and M. G. Pandy, "Sensitivity of muscle force estimates to variations in muscle–tendon properties," *Human movement science*, vol. 26, no. 2, pp. 306–319, 4 2007.

[26] M. Xiao and J. Higginson, "Sensitivity of estimated muscle force in forward simulation of normal walking," *J Appl Biomech*, vol. 26, no. 2, pp. 142–9, 2010.

[27] A. Navacchia, C. A. Myers, P. J. Rullkoetter, and K. B. Shelburne, "Prediction of in vivo knee joint loads using a global probabilistic analysis," *J Biomech Eng*, vol. 138, no. 3, p. 4032379, 2016.

[28] S. Delp, J. Loan, M. Hoy, F. Zajac, E. Topp, and J. Rosen, "An interactive graphics-based model of the lower extremity to study orthopaedic surgical procedures," *IEEE transactions on bio-medical engineering/IEEE transactions on biomedical engineering*, vol. 37, no. 8, pp. 757–767, 1 1990.

[29] A. G. Culvenor, M. A. Girdwood, C. B. Juhl, B. E. Patterson, M. J. Haberfield, P. M. Holm, A. Bricca, J. L. Whittaker, E. M. Roos, and K. M. Crossley, "Rehabilitation after anterior cruciate ligament and meniscal injuries: a best-evidence synthesis of systematic reviews for the OPTIKNEE consensus," *British Journal of Sports Medicine*, vol. 56, no. 24, pp. 1445–1453, 6 2022.

[30] "How static optimization works - OpenSim Documentation - OpenSim." [Online]. Available: https://opensimconfluence.atlassian.net/wiki/spaces/OpenSim/pages/53089619/How+Static+Optimization+Works

[31] "Joint Reactions Analysis - OpenSiM Documentation - OpenSim." [Online]. Available: https://opensimconfluence.atlassian.net/wiki/spaces/OpenSim/pages/53089600/Joint+Reactions+Analysis

[32] C. Lohmeijer, "Variation in muscle parameter values affecting tibiofemoral contact force during gait: a literature review," 2024.

[33] M. K. Horsman, H. Koopman, F. Van Der Helm, L. P. Prosé, and H. Veeger, "Morphological muscle and joint parameters for musculoskeletal modelling of the lower extremity," *Clinical biomechanics*, vol. 22, no. 2, pp. 239–247, 2 2007.

[34] M. D. McKay, R. J. Beckman, and W. J. Conover, "A Comparison of Three Methods for Selecting Values of Input Variables in the Analysis of Output from a Computer Code," *Technometrics*, vol. 21, no. 2, p. 239, 5 1979.

[35] K. Q. Ye, "Orthogonal column Latin hypercubes and their application in computer experiments," *Journal of the American Statistical Association*, vol. 93, no. 444, pp. 1430–1439, 12 1998. [Online]. Available: https://doi.org/10.1080/01621459.1998.10473803

[36] L. Bosmans, G. Valente, M. Wesseling, A. Van Campen, F. De Groote, J. De Schutter, and I. Jonkers, "Sensitivity of predicted muscle forces during gait to anatomical variability in musculotendon geometry," *Journal of Biomechanics*, vol. 48, no. 10, pp. 2116–2123, 3 2015.

[37] G. Valente, L. Pitto, D. Testi, A. Seth, S. L. Delp, R. Stagni, M. Viceconti, and F. Taddei, "Are Subject-Specific musculoskeletal models robust to the uncertainties in parameter identification?" *PLoS ONE*, vol. 9, no. 11, p. e112625, 11 2014. [Online]. Available: https://doi.org/10.1371/journal.pone.0112625

[38] D. G. Thelen and F. C. Anderson, "Using computed muscle control to generate forward dynamic simulations of human walking from experimental data," *Journal of Biomechanics*, vol. 39, no. 6, pp. 1107–1115, 7 2005.

[39] T. Wickiewicz, R. Roy, P. Powell, and V. Edgerton, "Muscle architecture of the human lower limb," *Clinical orthopaedics and related research*, pp. 275–283, 1983.

[40] J. A. Friederich and R. A. Brand, "Muscle fiber architecture in the human lower limb," *Journal of biomechanics*, vol. 23, no. 1, pp. 91–95, 1 1990.

[41] R. A. Brand, D. R. Pedersen, and J. A. Friederich, "The sensitivity of muscle force predictions to changes in physiologic cross-sectional area," *Journal of Biomechanics*, vol. 19, no. 8, pp. 589–596, 1 1986.

[42] "Xsens Knowledge base." [Online]. Available: https://base.movella.com/s/article/Gait-Report-How-to-interpret-data?language=en$_U S$

[43] B. Van Veen, E. Montefiori, L. Modenese, C. Mazzà, and M. Viceconti, "Muscle recruitment strategies can reduce joint loading during level walking," *Journal of Biomechanics*, vol. 97, p. 109368, 9 2019.

[44] D. D. D'Lima, S. Patil, N. Steklov, J. E. Slamin, and C. W. Colwell, "THE CHITRANJAN RANAWAT AWARD: In Vivo Knee Forces after Total Knee Arthroplasty," *Clinical Orthopaedics and Related Research*, vol. 440, no. NA;, pp. 45–49, 10 2005.

[45] D. D. D'Lima, S. Patil, N. Steklov, S. Chien, and C. W. Colwell, "In vivo knee moments and shear after total knee arthroplasty," *Journal of Biomechanics*, vol. 40, pp. S11–S17, 1 2007. [Online]. Available: https://doi.org/10.1016/j.jbiomech.2007.03.004

[46] S. Taylor, P. Walker, J. Perry, S. Cannon, and R. Woledge, "The forces in the distal femur and the knee during walking and other activities measured by telemetry," *The Journal of Arthroplasty*, vol. 13, no. 4, pp. 428–437, 6 1998.

[47] J. Morrison, "The mechanics of the knee joint in relation to normal walking," *Journal of Biomechanics*, vol. 3, no. 1, pp. 51–61, 1 1970.

[48] W. R. Taylor, M. O. Heller, G. Bergmann, and G. N. Duda, "Tibio-femoral loading during human gait and stair climbing," *Journal of Orthopaedic Research®*, vol. 22, no. 3, pp. 625–632, 11 2003.

[49] I. Kutzner, B. Heinlein, F. Graichen, A. Bender, A. Rohlmann, A. Halder, A. Beier, and G. Bergmann, "Loading of the knee joint during activities of daily living measured in vivo in five subjects," *Journal of Biomechanics*, vol. 43, no. 11, pp. 2164–2173, 6 2010.

[50] M. Bicer, A. T. Phillips, and L. Modenese, "Altering the strength of the muscles crossing the lower limb joints only affects knee joint reaction forces," *Gait and Posture*, vol. 95, pp. 210–216, 2022.

[51] C. Egloff, T. Hügle, and V. Valderrabano, "Biomechanics and pathomechanisms of osteoarthritis," *Schweizerische medizinische Wochenschrift*, 7 2012.

[52] S. Tanamas, F. S. Hanna, F. M. Cicuttini, A. E. Wluka, P. Berry, and D. M. Urquhart, "Does knee malalignment increase the risk of development and progression of knee osteoarthritis? A systematic review," *Arthritis Care Research*, vol. 61, no. 4, pp. 459–467, 3 2009.

[53] F. Maier, H. Drissi, and D. M. Pierce, "Shear deformations of human articular cartilage: Certain mechanical anisotropies apparent at large but not small shear strains," *Journal of the mechanical behavior of biomedical materials/Journal of mechanical behavior of biomedical materials*, vol. 65, pp. 53–65, 8 2016.

[54] A. D. Kaze, S. Maas, P.-J. Arnoux, C. Wolf, and D. Pape, "A finite element model of the lower limb during stance phase of gait cycle including the muscle forces," *BioMedical Engineering OnLine*, vol. 16, no. 1, 12 2017.

[55] S. Delp, "Surgery simulation: A computer graphics system to analyze and design musculoskeletal reconstruction fo the lower limb," Ph.D. dissertation, Stanford University, 1990.

[56] K. G. Gerritsen, A. J. Van Den Bogert, M. Hulliger, and R. F. Zernicke, "Intrinsic muscle Properties Facilitate Locomotor Control—A Computer Simulation study," *Motor control*, vol. 2, no. 3, pp. 206–220, 7 1998.

[57] A. J. Van Soest and M. F. Bobbert, "The contribution of muscle properties in the control of explosive movements," *Biological Cybernetics*, vol. 69, no. 3, pp. 195–204, 7 1993.

[58] E. M. Arnold, S. R. Ward, R. L. Lieber, and S. L. Delp, "A model of the lower limb for analysis of human movement," *Annals of biomedical engineering*, vol. 38, no. 2, pp. 269–279, 12 2009.

[59] S. R. Ward, C. M. Eng, L. H. Smallwood, and R. L. Lieber, "Are current measurements of lower extremity muscle architecture accurate?" *Clinical Orthopaedics and Related Research*, vol. 467, no. 4, p. 1074–1082, 2008.

[60] F. Mörl, T. Siebert, and D. Häufle, "Contraction dynamics and function of the muscle-tendon complex depend on the muscle fibre-tendon length ratio: a simulation study," *Biomechanics and Modeling in Mechanobiology*, vol. 15, no. 1, pp. 245–258, 6 2015.

[61] J. Goetschius, J. Hertel, S. A. Saliba, S. F. Brockmeier, and J. M. Hart, "GAIT biomechanics in anterior cruciate ligament–reconstructed knees at different time frames postsurgery," *Medicine Science in Sports Exercise*, vol. 50, no. 11, pp. 2209–2216, 6 2018.

[62] Q. Zhang, N. C. Adam, S. H. H. Nasab, W. R. Taylor, and C. R. Smith, "Techniques for in vivo Measurement of ligament and Tendon Strain: A review," *Annals of Biomedical Engineering*, vol. 49, no. 1, pp. 7–28, 10 2020.

[63] C. Winby, D. Lloyd, T. Besier, and T. Kirk, "Muscle and external load contribution to knee joint contact loads during normal gait," *Journal of biomechanics*, vol. 42, no. 14, pp. 2294–2300, 10 2009.

[64] J. Ojeda and J. Mayo, *A new approach to estimate a Subject-Specific set of muscle parameters*, 8 2012.

[65] K. B. Shelburne, M. R. Torry, and M. G. Pandy, "Muscle, Ligament, and Joint-Contact Forces at the Knee during Walking," *Medicine Science in Sports Exercise*, vol. 37, no. 11, pp. 1948–1956, 11 2005.

[66] F. C. Anderson and M. G. Pandy, "A dynamic optimization solution for vertical jumping in three dimensions," *Computer methods in biomechanics and biomedical engineering*, vol. 2, no. 3, pp. 201–231, 1 1999.

[67] M. G. Hoy, F. E. Zajac, and M. E. Gordon, "A musculoskeletal model of the human lower extremity: The effect of muscle, tendon, and moment arm on the moment-angle relationship of musculotendon actuators at the hip, knee, and ankle," *Journal of biomechanics*, vol. 23, no. 2, pp. 157–169, 1 1990.

[68] A. Rajagopal, C. L. Dembia, M. S. DeMers, D. D. Delp, J. L. Hicks, and S. L. Delp, "Full-Body musculoskeletal model for Muscle-Driven simulation of human GaIT," *IEEE transactions on bio-medical engineering/IEEE transactions on biomedical engineering*, vol. 63, no. 10, pp. 2068–2079, 10 2016.

[69] "ABAQUS Analysis User's Manual (V6.6)." [Online]. Available: https://classes.engineering.wustl.edu/2009/spring/mase5513/abaqus/docs/v6.6/books/usb/default.htm?startat=pt01ch01s02aus02.html

[70] C. Wan, Z. Hao, and S. Wen, "The finite element analysis of three grafts in the anterior cruciate ligament reconstruction," *Proceedings - 2011 4th International Conference on Biomedical Engineering and Informatics*, vol. 3, pp. 1338–1342, 10 2011.

[71] T. P. Andriacchi, P. L. Briant, S. L. Bevill, and S. Koo, "Rotational Changes at the Knee after ACL Injury Cause Cartilage Thinning," *Clinical Orthopaedics and Related Research*, vol. 442, pp. 39–44, 1 2006.

[72] L. Wang, L. Lin, Y. Feng, T. L. Fernandes, P. Asnis, A. Hosseini, and G. Li, "Anterior cruciate ligament reconstruction and cartilage contact forces—A 3D computational simulation," *Clinical Biomechanics*, vol. 30, no. 10, pp. 1175–1180, 8 2015.

[73] K. Halonen, M. Mononen, J. Töyräs, H. Kröger, A. Joukainen, and R. Korhonen, "Optimal graft stiffness and pre-strain restore normal joint motion and cartilage responses in ACL reconstructed knee," *Journal of Biomechanics*, vol. 49, no. 13, pp. 2566–2576, 5 2016.

[74] P. O. Bolcos, M. E. Mononen, A. Mohammadi, M. Ebrahimi, M. S. Tanaka, M. A. Samaan, R. B. Souza, X. Li, J.-S. Suomalainen, J. S. Jurvelin, J. Töyräs, and R. K. Korhonen, "Comparison between kinetic and kinetic-kinematic driven knee joint finite element models," *Scientific Reports*, vol. 8, no. 1, 11 2018.

A TSL reported in literature

Table 2: TSL values reported in literature

Muscle	Abbreviation	Min (cm)	Max (cm)
Adductor Brevis	add_brev	2 [55]	4.2 [66]
Adductor Longus	add_long	4 [67]	13.2 [68]
Adductor Magnus 1 (proximal)	add_mag1	4 [68]	12 [66]
Adductor Magnus 2	add_mag2	4.7 [68]	13 [55]
Adductor Magnus 3 (distal)	add_mag3	8.7 [68]	26 [55]
Biceps Femoris-Long Head	bifemlh	32.2 [58]	34.1 [55]
Biceps Femoris-Short Head	bifemsh	5 [66]	14 [66]
Erector Spinae	ercspn	3 [66]	3.11 [9]
Extensor Digitorum Longus	ext_dig	30 [66]	36.9 [68]
Extensor Hallucis Longus	ext_hal	26 [66]	33.2 [58]
fixme gem	gem	3.9 [58]	4.1 [9]
Flexor Digitorum Longus	flex_dig	37.8 [58]	39 [66]
Flexor Hallucis Longus	flex_hal	35.4 [68]	40 [55]
Gluteus Maximus 1 (lateral/superior)	glut_max1	4.9 [68]	10.6 [66]
Gluteus Maximus 2	glut_max2	6.8 [68]	7.3 [58]
Gluteus Maximus 3 (medial/inferior)	glut_max3	7 [68]	12 [66]
Gluteus Medius 1 (anterior)	glut_med1	3.5 [67]	7.8 [26]
Gluteus Medius 2	glut_med2	3.5 [67]	6.6 [58]
Gluteus Medius 3 (posterior)	glut_med3	3.5 [67]	5.3 [26]
Gluteus Minimus 1 (anterior)	glut_min1	1.6 [58]	5.51 [66]
Gluteus Minimus 2	glut_min2	2.5 [67]	2.6 [68]
Gluteus Minimus 3 (posterior)	glut_min3	4.8 [66]	5.1 [68]
Gracilis	grac	8 [67]	17.2 [68]
Iliacus	iliacus	8.5 [67]	14.2 [56]
Internal Oblique	intobl	10.3 [9]	16.5 [66]
Lateral Gastrocnemius	lat_gas	36 [26]	42.5 [67]
Medial Gastrocnemius	med_gas	36 [26]	42.5 [67]
Pectineus	pect	0.1 [66]	3.4 [9]
Peroneus Brevis	per_brev	14.8 [58]	30 [66]
Peroneus Longus	per_long	27.3 [67]	34.5 [55]
Peroneus Tertius	per_tert	10 [67]	30 [66]
Piriformis	peri	10.2 [66]	11.5 [68]
Psoas Major	psoas	8.5 [67]	14.2 [56]
Quadratus Femoris	quad_fem	2.4 [67]	2.5 [9]
Rectus Femoris	rect_fem	31 [9]	44.9 [68]
Sartorius	sar	4 [66]	12.4 [68]
Semimembranosus	semimem	33.4 [56]	37.8 [58]
Semitendinosus	semiten	24.5 [58]	33.4 [56]
Soleus	soleus	22 [26]	28.2 [58]
Tensor Fasciae Latae	tfl	42.5 [66]	45 [68]
Tibialis Anterior	tib_ant	22.3 [26]	31.7 [56]
Tibialis Posterior	tib_post	28.2 [58]	37 [66]
Vastus Intermedius	vas_int	10.6 [58]	20.2 [68]
Vastus Lateralis	vas_lat	13 [58]	22.1 [68]
Vastus Medialis	vas_med	11.2 [58]	20 [68]

B Unfiltered force data

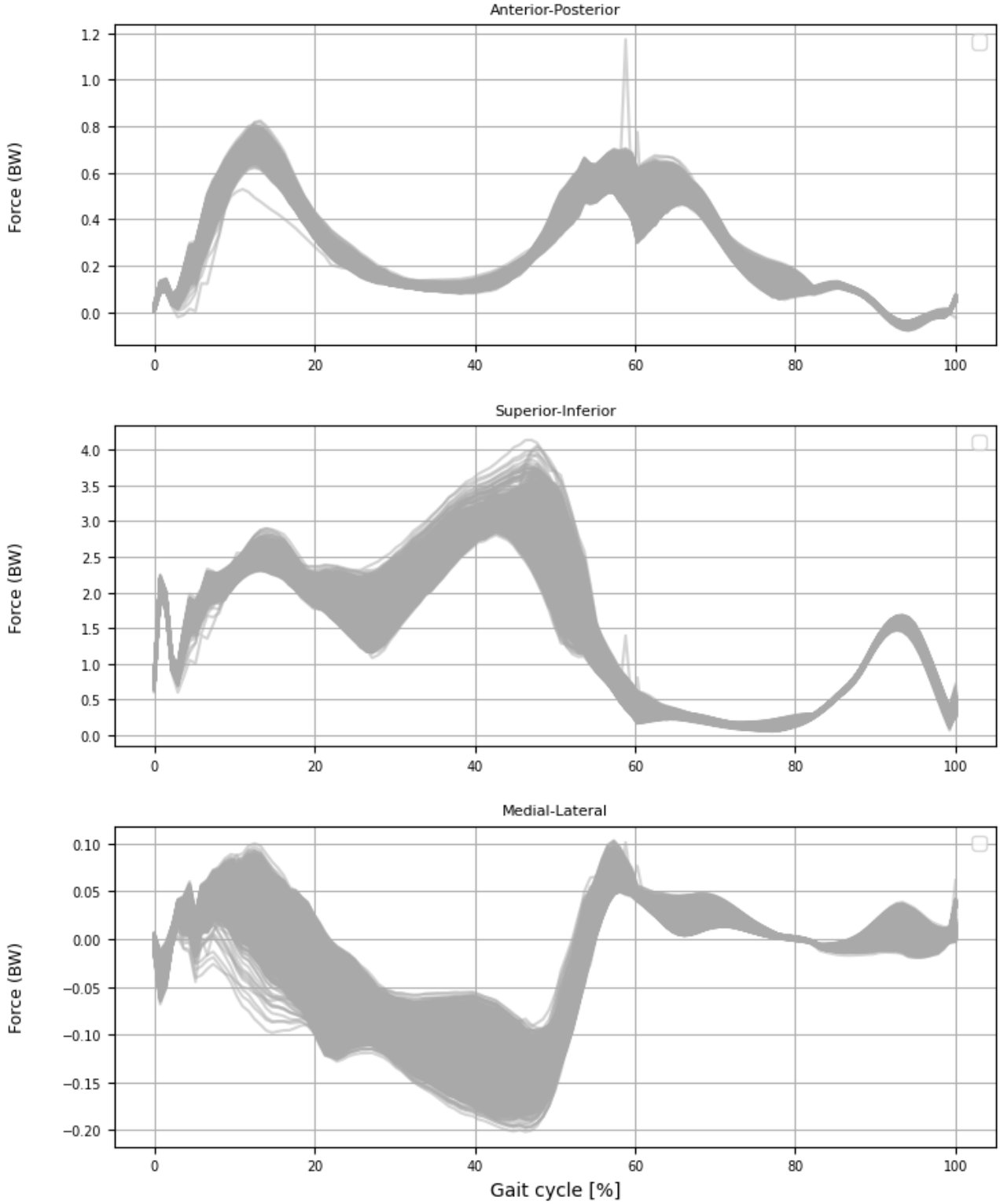

Figure 17: Unfiltered knee JRF estimations

C Workflow including results

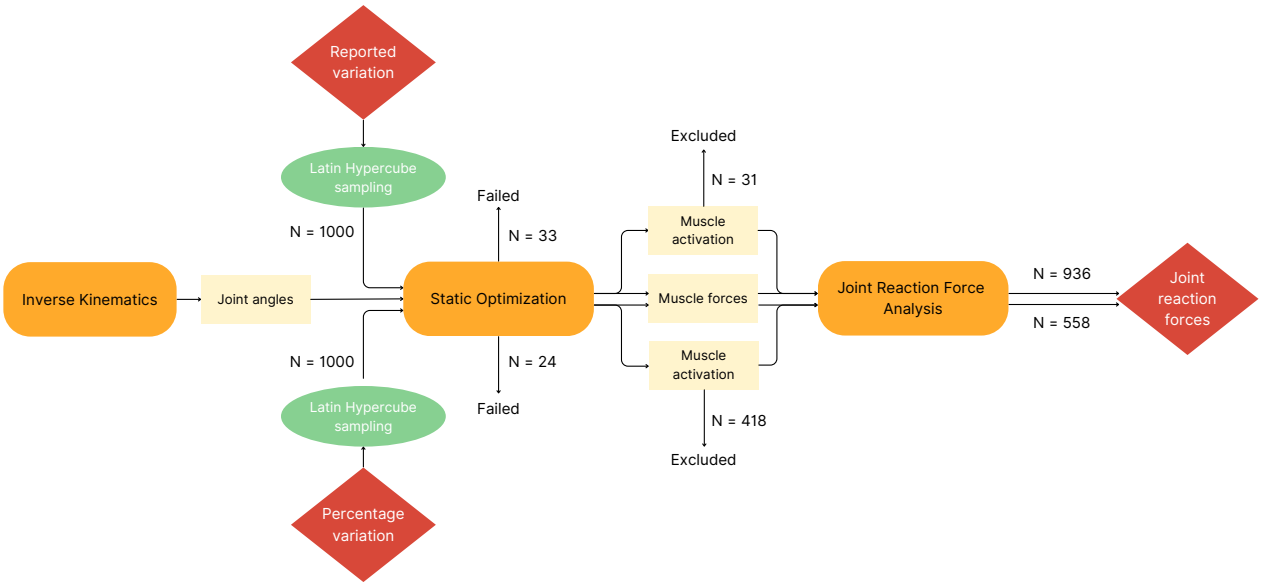

Figure 18: Workflow including simulations results

D Finite element modeling

D.1 Experimental set up

To investigate the effect of uncertainty in TSL on stress response in tibiofemoral AC, a FEM experiment was set up. The different simulations resulting from the MSM experiments formed the basis for the FEM experiment. Simulations with a different force pattern over the course of the gait cycle were selected. Each set of JRFs was meant to be used to run an FE simulation, while keeping the rest of input parameters the same. To this end, the JRFs of all simulations were investigated and three simulations with most deviating JRFs pattern over the gait cycle were selected as input models. The resulting stresses (Max, Min, Shear) were meant to give an indication of the effect of uncertainty in TSL on stress response in AC [69].

D.2 Model specifications

An existing FE knee model was used and adjusted to the demands of this research. The model consisted of the proximal end of the tibia and the distal end of the femur, including articular cartilage (AC) of both segments, and both menisci, see figure 19. The patella was not included. The ligaments were modeled as linear elastic springs, including anterior cruciate ligament (ACL) (reconstructed), posterior cruciate ligament (PCL), lateral collateral ligament (LCL) and medial collateral ligament (MCL) [70, 71, 72]. Stiffness of the cruciate ligaments were set to 20000 and 12000 for ACLR and PCL, respectively. Stiffness of the collateral ligaments was set to 10000 N/mm for both MCL and LCL [73, 74]. Young's Modulus was set to 17 MPa for AC and 59 MPa for the menisci. Poisson's ratio of both AC and menisci were set at 0.45.

Femur and tibia were modeled as discrete rigid parts and were assigned to the assembly as dependent instance types. A node-to-surface contact definition was assigned to the different assembly part. Reference points were based on center of mass onto which loading conditions were applied, containing one reference point both segments. Reference points for femur and tibia were modeled as point mass/inertia with an isotropic mass of 1. Reference points of the ligaments were based on origin and insertion, identified by means of segmentation.

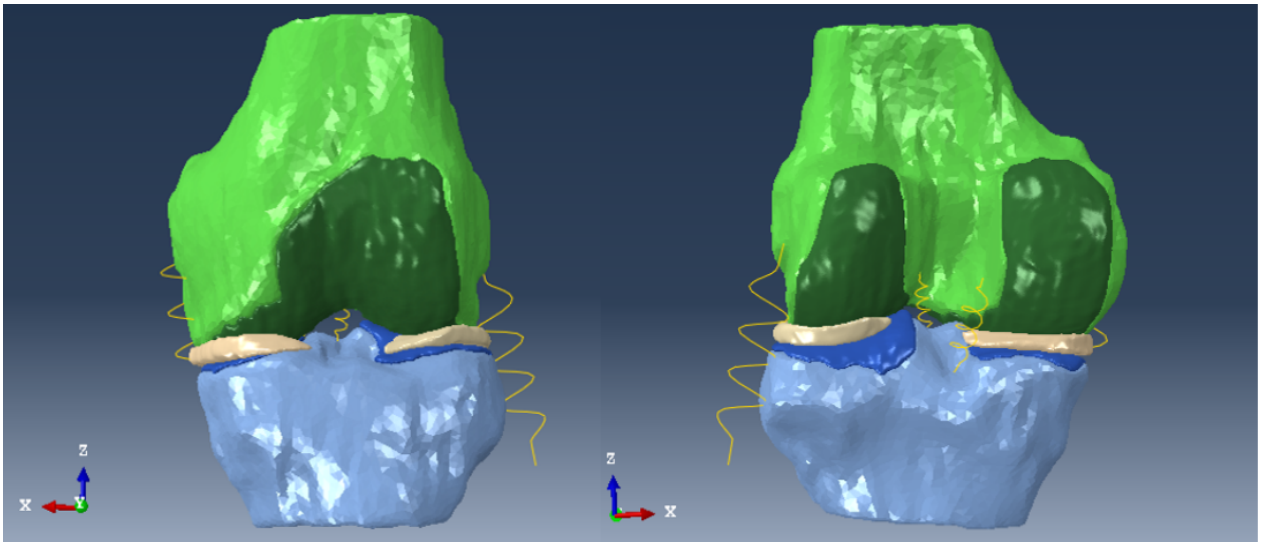

Figure 19: FE knee model, with tibia (blue) and tibial AC (dark blue), femur (green) and femoral AC (dark green). Menisci (light yellow) and ligaments yellow)

D.3 Gait simulation

The gait movement was modeled as a rotation of the femur with respect to the tibia. For that reason, the tibia and corresponding ligaments insertions were constricted in any translation or rotation by application of an encastre boundary condition. Menisci were also constrained using encastre boundary to prevent non-physiological movements. Medial-lateral translations and internal-external rotations were locked using displacement/rotation boundary conditions. Anterior-posterior translation, superior-distal translation and varus-valgus rotation were left open. Flexion angles during the simulated gait cycle were obtained from the IK tool in OpenSim. Since peak tibiofemoral forces are reached during the stance phase, it was decided to

limit the FEA to the stance phase of the gait cycle. The duration of the stance phase was retrieved from ground reaction force data from OpenSim, indicating a stance phase of 0.61 seconds.

The FEA was divided into three phases: pre-displacement, pre-loading and the gait cycle. The pre-displacement step was used to bring the tibia and femur to the starting flexion angle of the stance phase. The pre-loading step was used to ramp up the tibiofemoral force to the values assigned in the first time increment of the gait cycle step. The flexion angle was kept constant during this step. During the gait cycle step, each time increment a tibiofemoral force in x, y and z direction was applied to the elements corresponding to a certain flexion angle. The time for the pre-displacement and pre-loading step were left at default: 1 second (increment sizes, initial: 0.1, minimum: 1e-6, and maximum: 0.1). Initial increment sizes were reduced to 0.001 to improve convergence. (increment sizes, initial: 0.01, minimum: 61E-7, and maximum: 0.1).

For each FEA, the existing FE model was adjusted using Notepad++ and saved separately. JRFs were used as input for the FE model, containing force values for 80 time increments in x, y and z axis. A shell script was used to run the model on DHPC. A visual node on DHPC was used for visual inspection of the models.

D.4 Results

Variation in JRFs obtained through MSM simulations did not result in noticeable difference in stress response. Both the distribution of areas subjected to stress and the magnitude of the stress were equal over all simulations. It was reasoned that the ligament properties are too constraining for adjusted JRFs to show any effect on stress response. To test this hypothesis, the ligament stiffness was reduced with 90% and 900%. The simulation with reduced ligament stiffness of 900% led to instability in the system resulting in an uncompleted analysis due to convergence issues. The simulation with ligament stiffness reduced with 90% did run completely. Difference in vertical reaction forces of 0.8 x BW resulted in a difference in a peak compressive stress of 0.1 MPa. It was concluded that current FE knee model is not yet suitable for investigation of stress response as a result of variation in JRFs forces.